Section A-Research paper
ISSN 2063-5346

Enhancing Efficiency: Optimizing Charging and Discharging Times for Thermal Energy Storage Using Scheffler Solar Concentrators and Phase Change Materials

Varad Vichare[a*], Dr. Anita Nene[b], Ashish Utage[c]

[a] *PG Student, School of Mechanical Engineering, Dr. Vishwanath Karad MIT World Peace University, Pune, Maharashtra, India.*
[b] *Associate Professor, School of Mechanical Engineering, Dr. Vishwanath Karad MIT World Peace University, Pune, Maharashtra, India.*
[c] *Assistance Professor, School of Mechanical Engineering, Dr. Vishwanath Karad MIT World Peace University, Pune, Maharashtra, India.*
[a] *Corresponding author: varadvichare12@gmail.com /Orcid id: 0009-0007-4780-4929*

Abstract:

Thermal energy storage (TES) systems are crucial for bridging the energy supply-demand gap. While solar energy storage research has focused on flat-plate collectors, the potential of Scheffler solar concentrators remains largely unexplored. This study proposes an innovative approach using a Scheffler solar concentrator and phase change material (PCM) to address energy needs in rural areas with limited electricity access. Real-time testing with paraffin wax as the PCM and computational fluid dynamics (CFD) analysis were performed. The CFD analysis indicated a charging time of 17 minutes, and experimental results showed 18 minutes. This approach demonstrates feasibility in meeting the energy demands of rural communities. Using the response surface method, the optimal charging time was approximately 20.5 minutes, with an optimal discharging time of around 26.3 minutes. Paraffin wax was selected as the PCM due to its desirable thermal properties, such as high latent heat and low cost. The study clarifies that the proposed approach aims to address various energy needs in rural areas, including household heating, cooking, and water sterilization. The study highlights the potential of Scheffler solar concentrators and PCMs for sustainable and reliable TES, offering clean and accessible energy solutions to rural areas with limited electricity access.

Keywords: Thermal energy storage systems; Phase change material; Solar energy; Immersion water heater; RSM.

Nomenclature:

ρ	-	*Density.*
t	-	*Time.*
∇	-	*Dell operator.*
$\vec{V}$	-	*Velocity Vector.*
$T_{Liquidus}$	-	*Liquid phase temperature (◦C).*
$T_{Solidus}$	-	*Solid phase temperature (◦C).*
H	-	*Total Enthalpy.*
g	-	*Acceleration of gravity.*
$\emptyset$	-	*Porosity Value*

Abbreviations:

PCM	-	*Phase change Material.*
TES	-	*Thermal Energy Storage.*
CAE	-	*Computer Aided Engineering.*

1. Introduction

The increasing global energy demand has led to a growing reliance on non-renewable energy sources. However, renewable energy systems offer a potential solution to mitigate this dependence. Thermal energy storage systems have emerged as a promising technology to store and utilize excess energy from renewable sources like wind and solar power. These systems enable the collection and storage of heat energy, which can be used for heating, cooling, or converted back into electricity. In this context, the goal of this research is to address the need for water heating while reducing reliance on non-renewable energy sources. The project focuses on the development and testing of a portable solar immersion water heater that utilizes a latent heat energy system to store solar thermal energy. This approach aims to harness solar energy efficiently and facilitate its practical application for water heating purposes. Thermal energy storage systems collect and store heat energy, which can be utilized for various purposes such as heating, cooling, or converting back into electricity. One approach that is latent heat energy systems involve storing and releasing energy through phase transitions of a material, while sensible and latent heat storage refers to the combination of storing energy as both sensible heat (related to temperature change) and latent heat (related to phase change). Additionally, a Scheffler reflector is a type of solar concentrator used to focus sunlight onto a specific target.

By developing a portable solar immersion water heater that utilizes a latent heat energy system, this research aims to bridge the gap between renewable energy sources and water heating needs, contributing to a more sustainable and reliable energy future.

1.1. Literature Survey:

This paper discusses the challenges associated with the finite quantity and unpredictable prices of fossil fuels, as well as the contribution of their increased usage to global warming. Thermal energy storage (TES) systems, which store thermal energy for later use, are proposed as a solution, with a preference for latent heat storage due to their properties.

The energy generated from fossil fuels has fulfilled and served human needs for a long time (Joseph et al. 2016). However, the quantity of fossil fuels is finite, and their fluctuating prices make it unpredictable if an uninterrupted supply of energy is available. In addition, the increased use of traditional fossil fuels contributes significantly to global warming by releasing hazardous chemicals into the atmosphere. Future emissions brought on by unstable energy are predicted to quadruple. One approach is to use TES, or a Thermal Energy Storage system, to store the energy (Sharma et al. 2009). Simply put, this implies holding onto thermal energy for a predetermined period of time before using it. Both sensible and latent heat can be stored in order to accomplish this TES. Latent heat storage systems are chosen over sensible heat storage systems due to a number of factors, including high energy density, low storage density, and low cost (Himran, Suwono, and Mansoori 1994). These energy storage facilities increase the effectiveness of the energy systems and cut down on heat loss. Because it is abundant and close to the equator, solar energy is the ideal renewable energy source for a country like India (Sharma et al. 2009). The main goal of all modern research in this area has been to gather enormous amounts of solar energy and use it effectively for humanity (Babar, Arora, and Nema 2019). Use of the Scheffler reflector, a solar concentrator design with a fixed focus but just a single-axis tracking mechanism, is one of these well-known applications (Santosh Junare et al., 2017.). Because all solar heat flux is concentrated at a single fixed point, the reflector works simply by converting the incoming plane wave incident on the plane into a spherical wave that converges towards a fixed focus point. The single-axis sun tracking mechanism prevents this fixed point from being disturbed (Santosh Junare et al., 2017). (Babar, Arora, and Nema 2019) had completed work on selecting phase change materials for solar thermal storage applications. The study's goal was to choose an appropriate PCM as a thermal reservoir to be employed in a fat plate collector solar dryer. The low heat conductivity of PCM materials is one of their main disadvantages; however, employing nano-CuO at a concentration of 1% increases paraffin wax's thermal conductivity by 17.3% and decreases its melting time by 22.22% when compared to pure paraffin (en Zalba et al., n.d.). For the purpose of forecasting the transient behaviour of latent heat storage modules, numerous numerical models have been created. Phase change material (PCM) and Heat Transfer Fluid (HTF) are modelled as a one-dimensional system with a finite heat transfer coefficient, and both experimental and numerical results indicated some improvements in the charging and discharging rates (Dileep et al. 2021a). According to one study (Mahdi et al. 2021), hot water is delivered for a longer period of time in the morning at the expense of lower output temperatures. Calculations revealed that

PCM-mounted flat plate collectors could use the same quantity of hot water supply for a longer period of time. Moreover, one study (Trp 2005) came to the conclusion that the conductivity of the heat exchanger material had little effect on how quickly the PCM melts. The methodology followed during this study is explained in the terms of the flowchart given below in the [Figure 1], which includes the initial idea, followed by a detailed

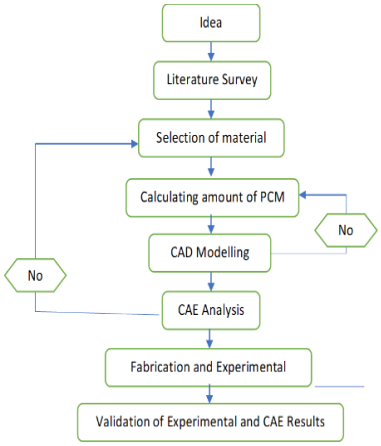

Fig.1 Research Methodology

research survey and then determining which phase change material is suitable for the application and rest of the analysis steps, which include CAE Analysis and experimental procedures. research survey and then determining which phase change material is suitable for the application and rest of the analysis steps, which include CAE Analysis and experimental procedures.

2. Scheffler Solar Concentrator:

The Scheffler solar concentrator is utilized in this research as a medium of heat source to provide the required heat supply for heating purposes. This concentrator design employs a single-axis tracking mechanism that maintains a fixed focus, enabling the concentration of all incoming solar heat flux at a single point. This is achieved by converting the incoming plane wave into a converging spherical wave, ensuring efficient concentration of solar energy. The simplicity of its working and the reliability of the single-axis tracking mechanism make it a promising solution for sustainable solar energy harvesting. For the current study, a Scheffler dish with an aperture area of 2.5 m2, a major axis of 2.200 m, and a minor axis of 0.830 m was utilized, based on available data (A. A. Nene, 2019). The Scheffler solar concentrator focuses the rays at a fixed point, known as the receiver point, as depicted in [Figure 2].

Fig2 Scheffler Solar Concentrator

The receiver point contains water that is heated up due to solar flux concentration, and the heated water is then supplied to the heater.

3. Selection of Phase change material:

Since that the heater's choice of material directly affects the system, it was essential for the heater to operate effectively. To achieve this, a phase change material (PCM) was used in accordance with the particular application, in this case water heating. Desired properties for material selection were identified, including the phase change temperature appropriate for the application, higher thermal conductivity, high latent heat of fusion, minimal density variation, affordability, abundance, non-toxicity, non-flammability, and non-polluting properties (Kabeel, El-Samadony, and El-Maghlany, 2018). With a focus on those that were easily accessible on the market and had a suitably high latent heat of fusion, a comparison research was carried out to evaluate various materials based on these required features. As the material needed to be handled regularly, non-toxicity and easy availability were prioritized. Several PCM options were considered for the project, as presented in [Table 1]

Properties	**Lauric Acid**	**Paraffin wax**	**Steric Acid**
Latent heat of fusion	170 KJ/Kg	206 KJ/Kg	199 KJ/Kg
Melting Point	44^0 C	75^0 C	69^0 C
Toxicity	Non-Toxic	Non-Toxic	Non-Toxic

Table 1 Material Comparisons

Ultimately, paraffin wax was selected as the heat storage material, as it is a type of straight chain alkane or n-alkane (Ukrainczyk et al., 2010) that is non-toxic, non-corrosive, and affordable. Depending on the application and the melting point of the paraffin wax, a specific type of paraffin wax was chosen. As the desired water heating temperature range was 55-65°C, a suitable paraffin wax was selected accordingly. The properties of the chosen paraffin wax are provided in [Table 2].

Sr no.	Parameters	Values
1	Melting point	58^0 C to 62^0 C.
2	Latent heat of fusion(kJ/kg)	195
3	Thermal Conductivity	0.24W/m K
4	Density(kg/m^3)	900

Table2 Paraffin Properties

4. Experimental Test rig:

The current study's goal was to examine the thermal performance of a small, effective shell and tube heater. The heater was designed according to and had an outer shell with a length of 0.6 m, outer diameter of 0.2256 m, and wall thickness of 0.0032 m. The inner tube had a length of 0.4 m, outer diameter of 0.1717 m, and wall thickness of 0.00254 m. The overall capacity of the shell to hold water was 13.54 liters, and the tube could carry about 7.35 kg of phase change material. A 1:2 scale model was prepared for lab testing purposes based on the actual dimensions. The measurement of temperatures inside the heater was achieved using thermocouples, and a MATLAB code was programmed for the estimation of dimensions. An insulation material, PUF (Poly-urethane foam) with a conductivity of 0.03 W/m K and a density of 24 kg/m3 (Mahdi et al., 2021), was selected to reduce heat loss from the shell. A CAD model of the design parameters was also created in SOLIDWORKS software for simulation purposes which is shown in [Figure 3].

ISSN 2063-5346

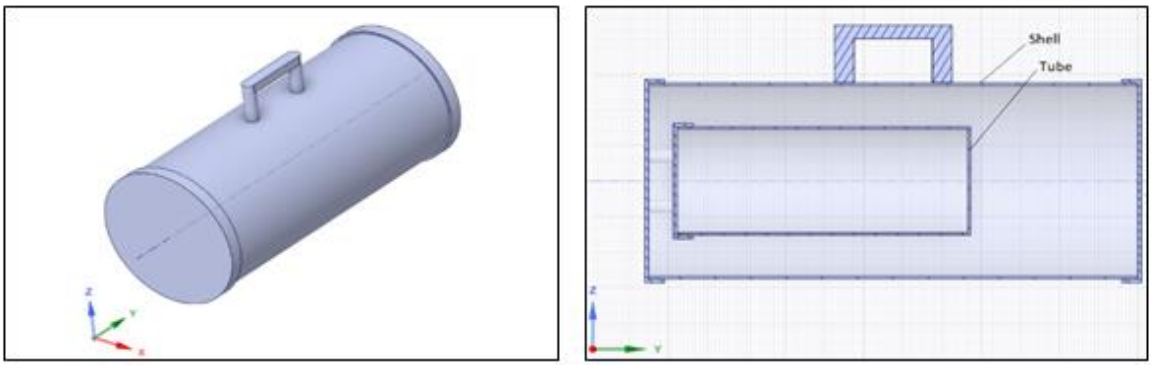

Fig 3 Thermal Energy Capsule

The thermal capsule contained a shell, water jacket, tube, and phase change material. The receiver, which contained 8 liters of water, was heated using a Scheffler solar concentrator. The high-temperature water was then sent to the thermal storage capsule, where it charged the phase change material. The heated tube could then be removed and used to heat water by discharging the stored thermal energy.

4.1. Experimental Procedure:

The experimental setup consisted of a shell and a tube, wherein a scaled model was utilized for laboratory testing. Prior to conducting the experiment, a phase change material was filled inside the aluminum tube and thermocouples were placed at three points in the outer periphery and center of the tube to measure the temperature of the material. The initial condition of the phase change material was determined when all thermocouples recorded the same temperature, and measures were taken to prevent any leakage from the sealed aluminum tube. Heated water at 90°C was then poured inside the shell, and its temperature was monitored by a thermocouple. Temperature readings were recorded every 60 seconds for all thermocouples until a constant value was obtained for all readings, indicating the completion of the charging phase. Simultaneously, the temperature of the water in the shell was also measured. The discharging phase began with the initial conditions established during the charging phase, and the charged aluminum tube was then inserted into a container of water at ambient temperature. The same experimental procedure was followed as during the melting process, and the solidification process was considered complete when every thermocouple in the paraffin and container recorded the same temperature value.

5. Numerical Analysis:

The process of conducting an analysis of a heater using Ansys Fluent involves several steps that can be depicted using a flowchart which is shown in [Figure 4]. Firstly, a 2D geometry of the heater tube is prepared using the DESIGN MODELER software in Ansys Workbench, and named selections are made for each face. Next, the computational mesh is generated in Ansys Meshing software, using various methods such as patch conforming and inflation to improve the quality of the mesh. For the numerical analysis of heat transfer and fluid dynamics, the governing equations, including the continuity equation, momentum equation, and energy equation, are used under the assumptions of laminar flow and constant thermophysical parameters. Natural convection in the ETC tubes is taken into account using the Boussinesq approximation, and the phase transition process is modelled using the enthalpy porosity technique. The pressure, time derivative terms, momentum, and energy equations are solved using the laminar model once the boundary conditions are established for the temperatures of each wall.

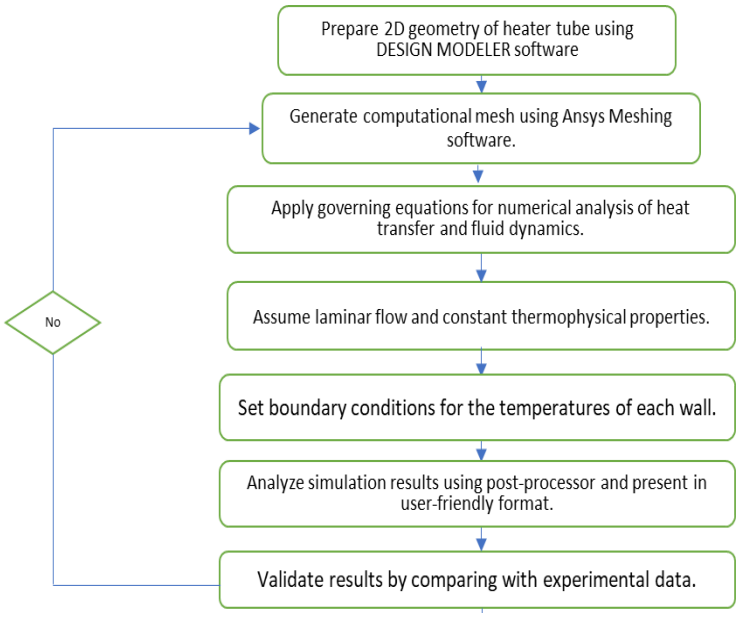

Fig4: Flow chart

Numerical discretization is performed using temporal schemes and second-order upwind schemes, and under-relaxation parameters are modified to improve convergence accuracy while reducing calculation time. Finally, the simulation results are analysed using a post-processor and presented in a user-friendly format.

5.1. Validation:

The results obtained from the Computational Fluid Dynamics (CFD) analysis were compared with experimental

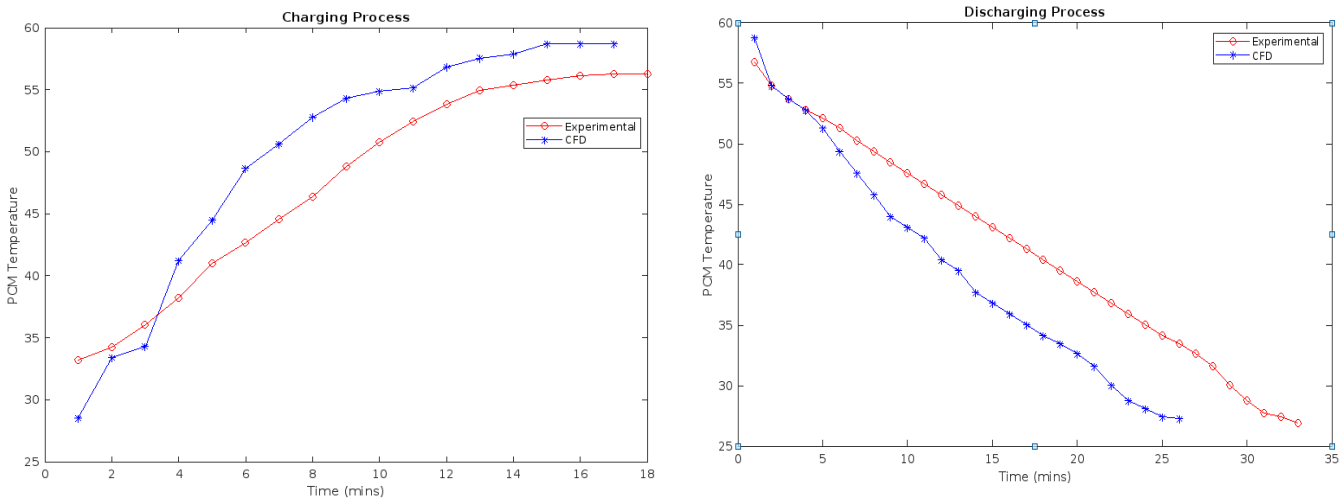

results, as depicted in [Figure 5] below

Fig5 Experimental and CFD comparison

Between the numerical and experimental data, a respectable level of agreement was seen. The discrepancy between the CFD and experimental data during the charging process was found to be 5.5%, whereas, during the discharging process, the overall deviation was approximately 15%. These deviations are deemed acceptable for both scenarios.

5.2. Uncertainty Analysis:

Uncertainty analysis is an important consideration when evaluating the effectiveness and reliability of the proposed approach for energy storage. One possible source of uncertainty is the use of paraffin wax as the PCM, which may have different properties and behaviors than other PCMs. Additionally, the use of thermocouples for temperature measurement can introduce uncertainties due to several sources, including non-uniform temperature distribution, thermocouple calibration. To estimate these uncertainties, thermocouples used during the experiment are calibrated using a reliable reference thermometer or temperature source. Additionally, statistical analysis techniques, such as Monte Carlo simulation, used to quantify the uncertainty in the charging and discharging times and to evaluate the robustness of the system under different operating conditions and scenarios.

6. Optimization of Charging and Discharging time:

Statistical methodology known as Response Surface Methodology (RSM) uses a mathematical model to maximize response variables by modifying controllable process factors. This technique reduces the need for expensive and complex analysis methods such as finite element method or CFD analysis, which can be costly and have numerical noise. RSM is an efficient and cost-effective tool for minimizing analysis costs.

6.1.1. Design Of Experiment:

For optimization of charging time water temperature and heating time of water were consider as the two variables. Design matrix is given in [Table 3].
For Solar portable immersion heater, the correlations obtained for input and response are:

1. Water temperature vs Charging time = -0.954.
2. Heating Time vs Charging time = -0.029.

ISSN 2063-5346

Run	Factor 1 A: Water Temperature ^{0}C	Factor 2 B: Heating Time mins.	Response 1: Charging Time mins.
1	80	16.9	21
2	64	21.8	35
3	64	12	35
4	80	16.9	21
5	80	16.9	21
6	80	16.9	21
7	96	21.8	15
8	80	23.8	18
9	96	12	12
10	80	16.9	21

Table 3 Design Matrix (DOE)

The above-mentioned correlations can be shown in the [Figure 6] below, the negative value of correlation

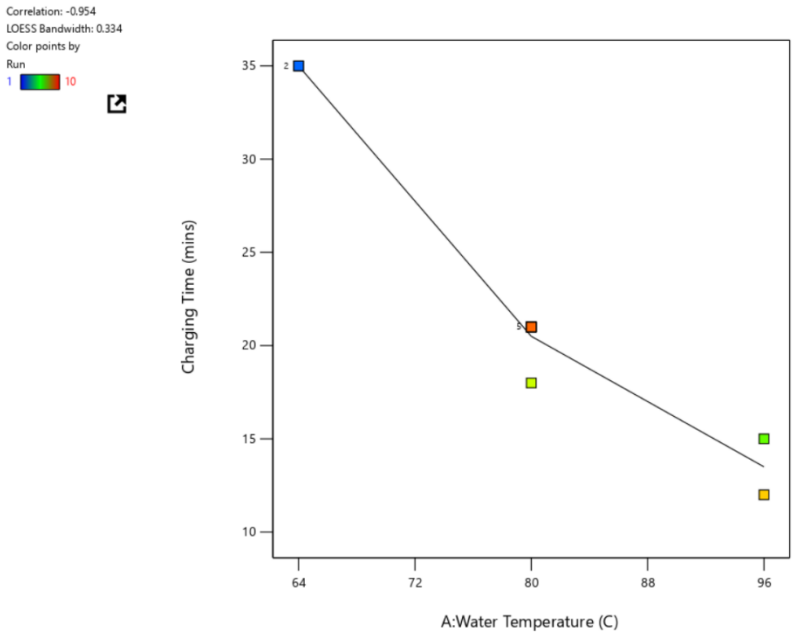

suggests that as the water temperature is going to get increase the charging time is going to go down.

Fig6 Correlation Graph

Likewise, as the heating time of water is going to rise as a result it will increase the water temperature and, ultimately will decreases the charging time. The Standard error design graph reflects that the design points are in

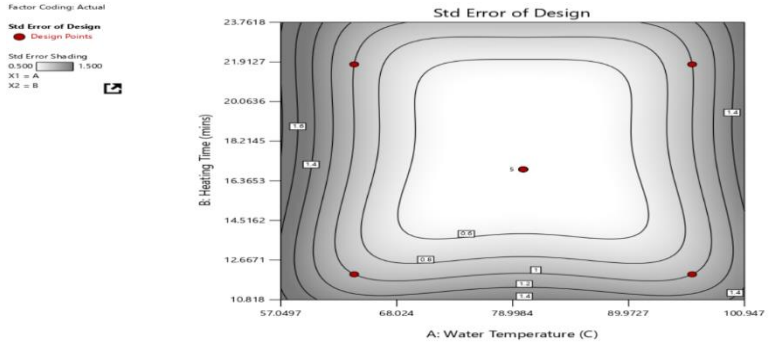

the range between 0.50% to 1.50% of error. It can be seen in the below [Figure 7].

Fig7 Standard error design graph

6.1.2. Analysis:

In the current case, no transformation is required as the requirement of transformation arises when the value of ratio of minimum range of response to maximum range of response is less than 10 in this case which it is. Then after available models are compared on the basis of R^2 value, higher the value of R^2 is desirable so the model having a high value of R^2 is selected. The below [Table 4] suggested the values of R^2 for different model,

Source	Std Dev.	R^2	Adjusted R^2	Predicted R^2	PRESS	
Linear	2.52	0.9123	0.8873	0.7196	142.47	**Suggested**
2FI	2.65	0.9168	0.8751	0.1956	408.66	
Quadratic	0.0000	1.0000	1.0000			
Cubic						

Table 4 R^2 Values

According to the fit summary, the Linear model is the best fit model since it has the greatest Predicted and Adjusted R2 value and a standard deviation of 2.52. The analysis of variance [Table 5] demonstrates that the model F-value of 36.43 implies that the model is significant, since there is only a 0.02% probability that the model is unimportant.

Source	Sum of Squares	dF	Mean Square	F-value	p-value	
Model	463.47	2	231.73	36.43	0.0002	**Significant**
A- Water Temperature	462.25	1	462.25	72.66	< 0.0001	
B- Heating Time	1.222	1	1.22	0.1913	0.6750	
Residual	44.53	7	6.36			
Lack of fit	44.53	3	14.84			
Pure Error	0.0000	4	0.0000			
Cor Total	508.00	9				

Table 5 ANOVA Results

Model terms are significant when the P-value is less than 0.0500. A are key model terms in this scenario. Value greater than 0.1000 implies the model terms are not significant. Model reduction may enhance your model if there are numerous unimportant model terms present.

General Equation:

The following general equation can be used in order to predict the response value:

$$Charging\ time = 77.39468 - 0.671875 \times T_{water} - 0.093485 \times Heating_{Time}$$

The predicted vs actual graph shows that a good agreement can be seen in the values of the predicted response and actual response. It can be seen in the [Figure 8].

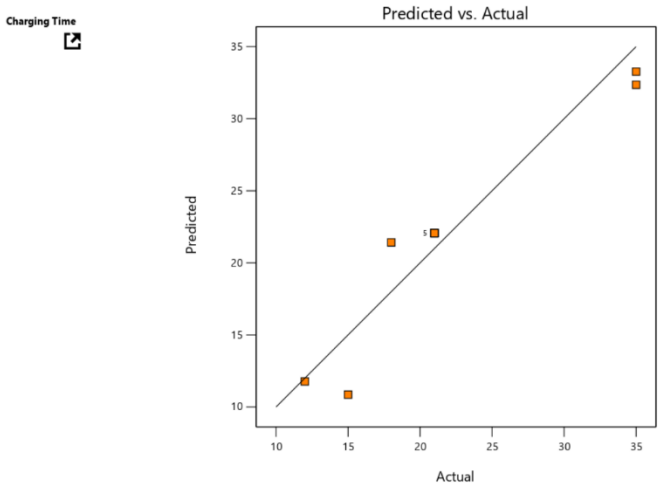

Fig 8: Predicted vs Actual

The model graph shown in [Figure 9] shows the region of maximum to minimum value of the response surface. The area with the highest response value is highlighted in red, while the area with the lowest response value is highlighted in blue.

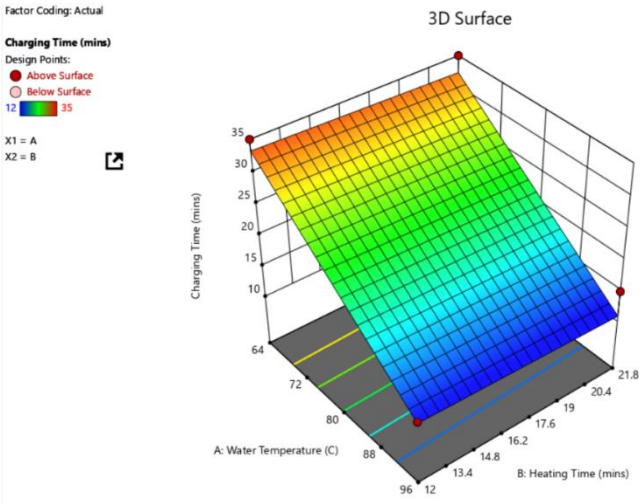

Fig 9: 3D Surface for Charging Time

7. Results and Discussion:

This study aims for the designing and analysing a solar portable immersion water heater, Solar thermal energy is stored in the form of a latent heat energy system. The results obtained from both CFD and experimental are explained below.

7.1. Experimental Results for Charging and Discharging:

Experimental results obtained for charging and discharging process are shown in the [figure 10],

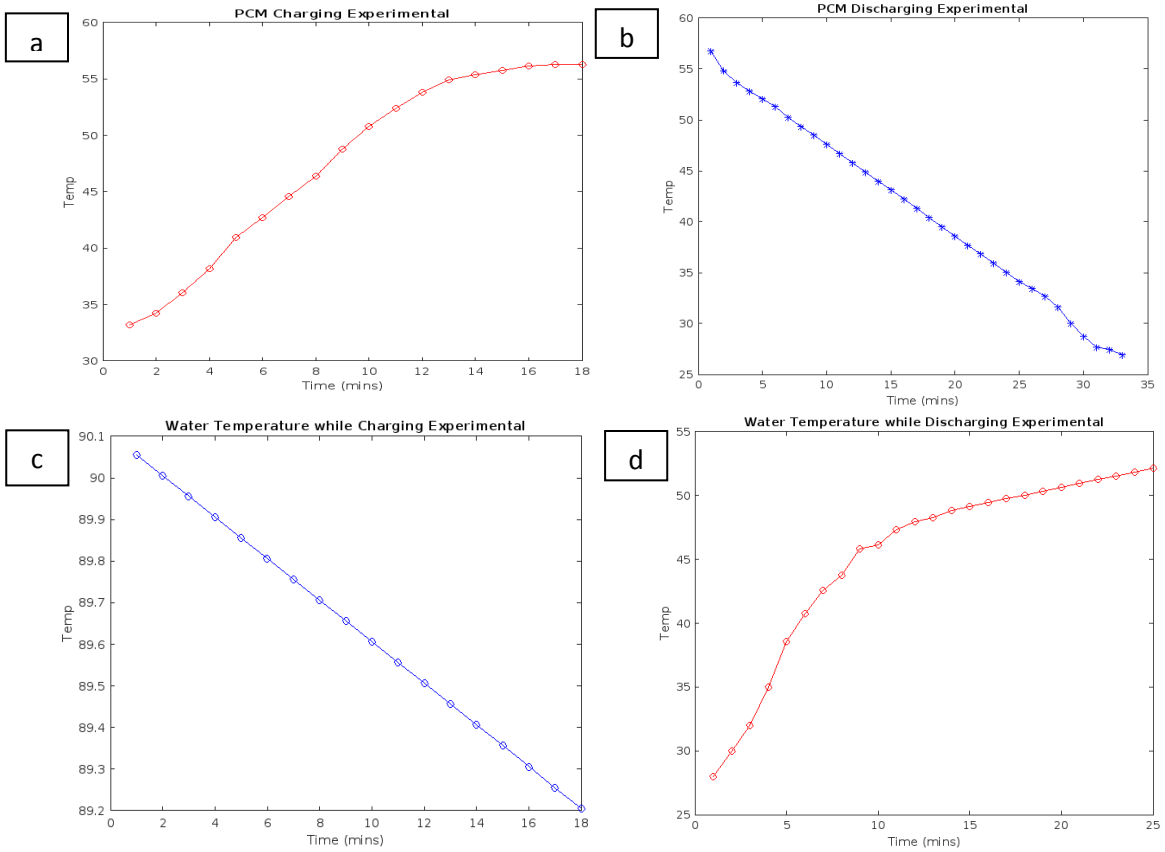

Fig10 Experimental Results for charging and Discharging

[Figure 10 (a)] shows the changes in the PCM temperature as it changes from below 30°C to 56°C. The water temperature outside the PCM tube was maintained in the temperature range of 90-89^{0}C, as seen in [Figure 10 (c)]. During the experimental approach, maintaining a constant water temperature of 90°C was not maintained due to heat losses, mainly occurring in a radially outward direction. Also, in the case of the PCM temperature, the results showed a fair conversion at the temperature of 56.2°C instead of showing it between 58°C – 62°C. This could be due to the impurities present inside the material. The total charging time required for the complete melting of paraffin experimentally was found to be 18 minutes. In case of discharging process, experimental results recorded a significant increase in the water temperature, from 37.20^{0}C to 52.50^{0}C, while the paraffin wax's temperature dropped from 55.80^{0}C to 27.40^{0}C. This was due to the transfer of energy from the higher temperature region of the PCM tube to the water, which was at a lower temperature. The temperature behaviour of the PCM and water is shown in the graphs (b) and (d) respectively in [Figure 10]. The PCM temperature exhibited linear behaviour up until the 30-minute mark, after which it flattened out, indicating the convergence of results. In contrast, the water temperature graph showed a gradual increase at the start, followed by a sudden elevation in the middle before converging to a temperature of 52.20C. This sudden elevation could be due to external factors affecting the heat transfer process, resulting in deviations in the temperature values. The total time required for the discharging phase to complete experimentally was found to be 32 minutes. The experimental results depicting the condition of paraffin wax during charging and discharging process is shown in [Figure 11 a &b].

(a) **(b)**

Fig11 (a) Discharged PCM (b) Charged PCM

7.2. CFD Results for Charging and Discharging:

Results obtained from CFD analysis for charging and discharging process are shown in the [figure 12]

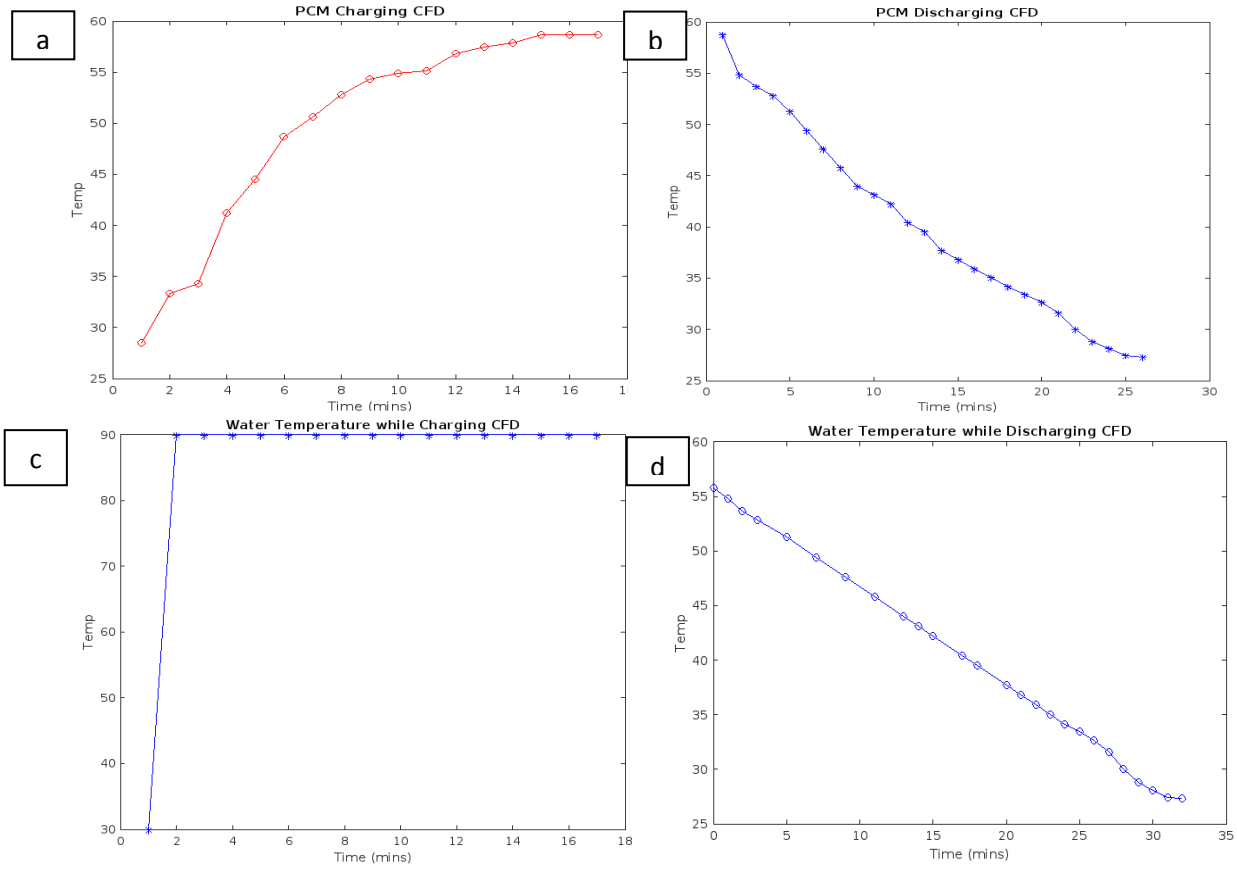

Fig12 CFD results for charging and Discharging

The numerical analysis recorded a charging time of 17 minutes for the complete melting of paraffin wax when the maintained at a constant condition of water at temperature of 90°C, as seen in [Figure 12 (c)]. [Figure 12 (a)]

shows the changes in the PCM temperature as it changes from below 27°C to 58°C. The starting or usual paraffin wax conditions were set at 30°C, and the paraffin wax was in the solid phase. Nonetheless, the temperature observed at the end of the charging operation was 58.7°C, indicating that the paraffin was in the liquid phase. The total charging time required for the complete melting of paraffin from the numerical analysis was recorded as 17 minutes. In case of discharging process, the numerical analysis performed on the same system, recorded discharging time for complete solidification of paraffin wax was about 26 minutes. The results obtained through numerical analysis were obtained under constant boundary conditions and without any interference from external factors, unlike the experimental results. The temperature distribution of paraffin and water is shown in graphs (b) and (d) in [Figure 12], respectively, where the temperature of the paraffin wax decreased from 59^0C to 27.20^0C as it released energy to the water, resulting in an increase in the water temperature from 37.20^0C to 53^0C. The behavioral changes recorded in the case of paraffin material in its temperatures and liquid fractions at different melting times can be seen in [Figure 13].

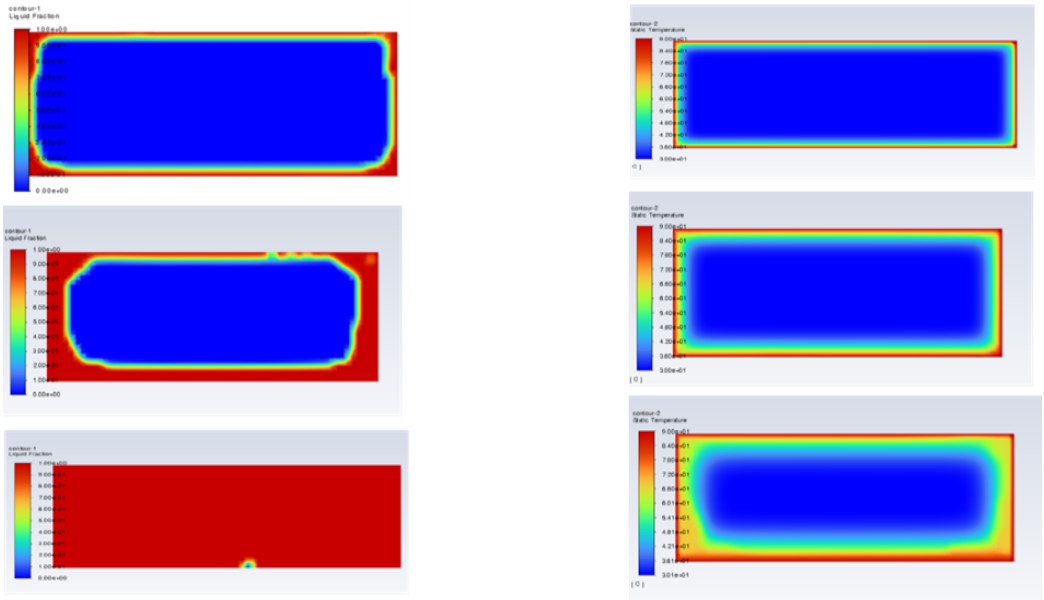

1. **(b)**

Fig13 CFD Temperature and Liquid fraction contours

The figures reflect the minute changes through which the paraffin wax undergoes as time passes. The figure shows the way in which the paraffin gets melted, starting with the melting of the outer regions of the paraffin and then getting melted to its center. The value of 0 indicates the solid state and the value of 1 indicates the full melting of PCM. The results for liquid fractions are generally calculated to understand the changes that happen in the phase of a material. The temperature contours in [Figure 13] show the behavioral conditions of convection currents that are formed due to the rise in the temperature of PCM, owing to heat transfer. Where part (a) represents the changes that take place during the melting, as how PCM is going to get melted as time passes. The figure clearly shows that the melting will first start from the outside region of the PCM and then will converge inside as it is expected with the presence of a wall temperature of 90^0C. Whereas part (b) in [Figure 13] shows the temperature changes which are going to take place inside the PCM as it is exposed to a constant temperature of 90^0C. The variation in liquid fraction and the temperature have proportionality with each other as the increase in the temperature will result in the melting of the PCM.

ISSN 2063-5346

7.3. Optimization Results for Charging and Discharging:

The results of the experiments demonstrate that the charging time is maximum when the water temperature is low and then after varies with the increase in temperature but at a same time heating also tends to vary with changes in water temperature. As a result, it is necessary to carry out optimization for different values of water temperature. In this case, the optimization has been done for the charging time at different water temperature and heating time. The results of optimum charging time can be seen in the [Figure 14].

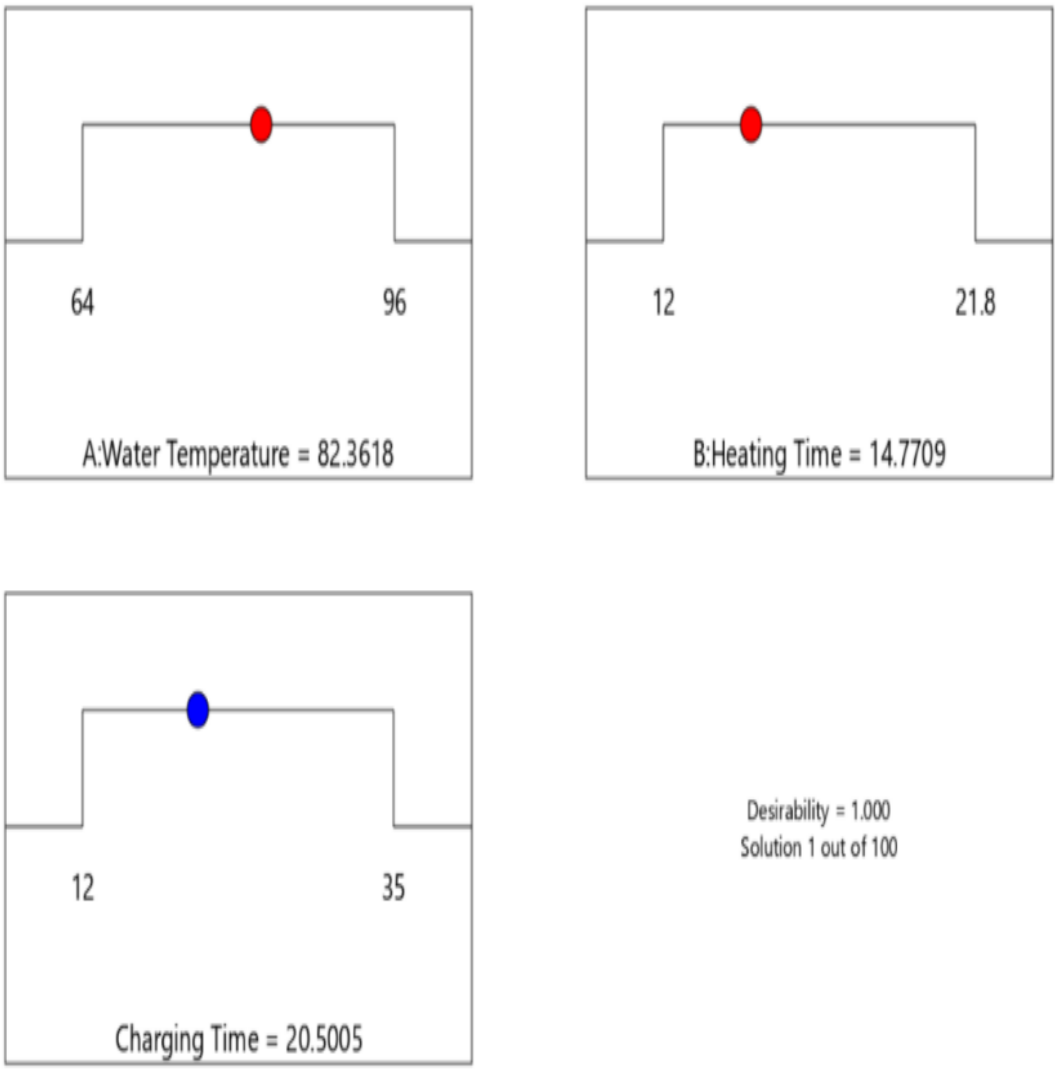

Fig14 Ramps for Charging Process

Optimal charging time varies from 12 to 35 mins. In this case charging time is 20.5005 mins with 95% confidence level for water temperature of 82.3618^{0}C and for a heating time of 14.7709 mins. The corresponding graphical optimization is shown in [Figure 15].

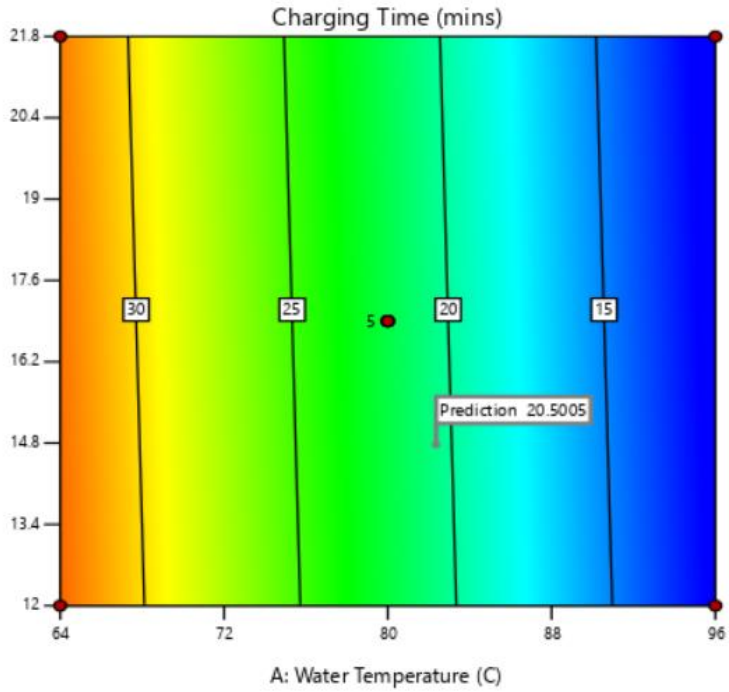

Fig 15: Charging Time Optimization Graph

In case of discharging process the findings of the experiment revealed that the discharging time is maximum for the water which was present at higher temperature, where as it decreases as the water poured inside is of low temperature. This might be owing to the fact that the heat transfer rate of higher temperature water is much lower than that of lower temperature water, as delta T is more in later case. In this case, the optimization has been done for the discharging time at different initial water temperature and different water temperature. The results of optimization can be seen in the [Figure 16]

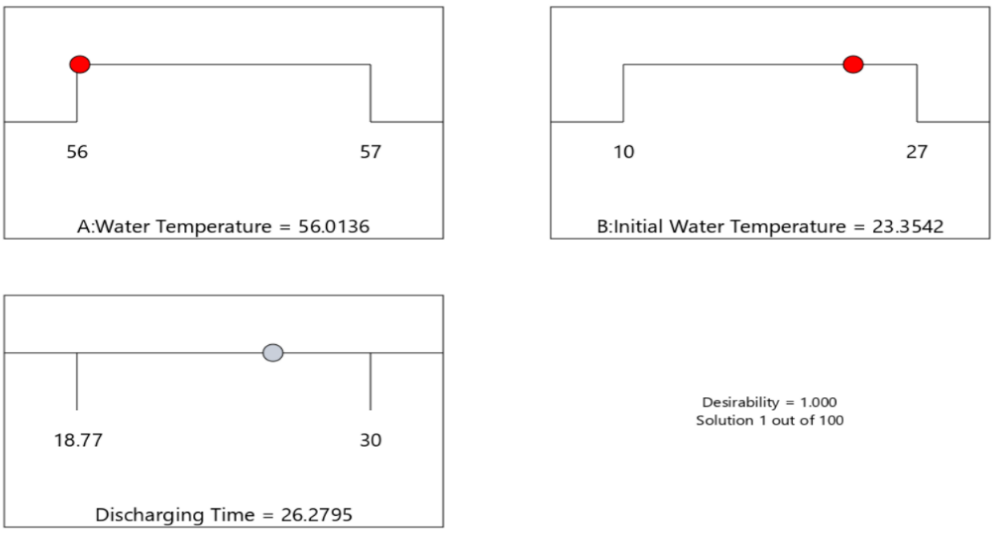

Fig16 Ramps for Discharging Process

Optimal discharging time varies from 18.77 to 30 mins. In this case optimal discharging time is 26.2795 mins with an optimal water temperature as 56.01^0C and initial water temperature as 23.35^0C. The corresponding graphical optimization is shown in [Figure 17]

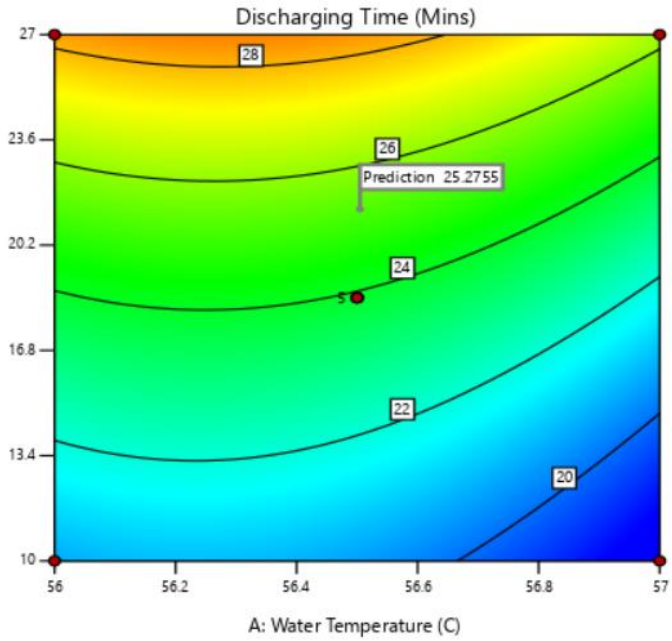

Fig17 Discharging Time Optimization Graph

8. Conclusion:

In this study, a comprehensive numerical and experimental analysis was conducted to investigate the performance of a thermal energy storage system utilizing a Scheffler Solar Concentrator and phase change material.

1. Results from the CFD analysis indicated that the PCM required 17 minutes to fully charge and 26 minutes to fully discharge.
2. Experimental tests demonstrated that the charging time was 18 minutes and the discharging time was 32 minutes.
3. While a deviation of 5.55% was observed in the charging phase and 15% in the discharging phase, this deviation must be due to the heat losses, presence of impurities in PCM, errors in measuring devices, and other external factors.
4. Uncertainty analysis is important for evaluating the reliability of energy storage methods, including potential sources of error from the use of paraffin wax as a PCM and thermocouple measurement.
5. Optimal charging time found is 20.5 mins for water temperature of 82.3618^0C and heating time of 14.7701 mins and the optimal discharging time is 26.2 mins for water temperature of 56.0136^0C and a surrounding water temperature of 23.3542^0C.

This research has demonstrated the potential of using Scheffler solar concentrators and phase change materials for thermal energy storage, which can be a cost-effective and sustainable solution for meeting the energy demands of rural areas with limited access to electricity.

Acknowledgment:

I would like to thank Dr. A. A. Nene and Mr. Ashish Utage for their experience and support throughout all phases of our investigation, as well as their aid in authoring the paper.

References:

Babar, Onkar A., Vinkel K. Arora, and Prabhat K. Nema. 2019. "Selection of Phase Change Material for Solar Thermal Storage Application: A Comparative Study." *Journal of the Brazilian Society of Mechanical Sciences and Engineering* 41 (9). https://doi.org/10.1007/s40430-019-1853-1.

Chiranjeevi Naidu, Gali, K Dharma Reddy, and P v Ramaiah. n.d. "CFD Simulation for Charging and Discharging Process of Thermal Energy Storage System Using Phase Change Material." https://doi.org/10.17950/ijer/v5s4/426.

Dileep, K., K. R. Arun, D. Dishnu, M. Srinivas, and S. Jayaraj. 2021a. "Numerical Studies on the Effect of Location and Number of Containers on the Phase Transition of PCM-Integrated Evacuated Tube Solar Water Heater." *Journal of Thermal Analysis and Calorimetry* 143 (1): 737–49. https://doi.org/10.1007/s10973-019-09151-2.

———. 2021b. "Numerical Studies on the Effect of Location and Number of Containers on the Phase Transition of PCM-Integrated Evacuated Tube Solar Water Heater." *Journal of Thermal Analysis and Calorimetry* 143 (1): 737–49. https://doi.org/10.1007/s10973-019-09151-2.

en Zalba, Bel, Jos M Mar ı ın, Luisa F Cabeza, and Harald Mehling. n.d. "Review on Thermal Energy Storage with Phase Change: Materials, Heat Transfer Analysis and Applications." www.elsevier.com/locate/apthermeng.

"Full Thesis with All Documents 13th August 2020 (1)." n.d.

Himran, S, A Suwono, and G A Mansoori. 1994. "Characterization of Alkanes and Paraffin Waxes for Application as Phase Change Energy Storage Medium Energy Sources." Vol. 16.

Joseph, Alain, Moe Kabbara, Dominic Groulx, Paul Allred, and Mary Anne White. 2016. "Characterization and Real-Time Testing of Phase-Change Materials for Solar Thermal Energy Storage." *International Journal of Energy Research* 40 (1): 61–70. https://doi.org/10.1002/er.3336.

Kabeel, A. E., Y. A.F. El-Samadony, and Wael M. El-Maghlany. 2018. "Comparative Study on the Solar Still Performance Utilizing Different PCM." *Desalination* 432 (April): 89–96. https://doi.org/10.1016/j.desal.2018.01.016.

Mahdi, Mustafa S., Hameed B. Mahood, Ahmed A. Alammar, and Anees A. Khadom. 2021. "Numerical Investigation of PCM Melting Using Different Tube Configurations in a Shell and Tube Latent Heat Thermal Storage Unit." *Thermal Science and Engineering Progress* 25 (October). https://doi.org/10.1016/j.tsep.2021.101030.

Santosh Junare, Somesh, Shubham Vilas Zamre, and Monika Madhukar Aware. n.d. "Scheffler Dish and Its Applications," 2017. http://www.ijritcc.org.

Sharma, Atul, V. v. Tyagi, C. R. Chen, and D. Buddhi. 2009. "Review on Thermal Energy Storage with Phase Change Materials and Applications." *Renewable and Sustainable Energy Reviews*. https://doi.org/10.1016/j.rser.2007.10.005.

Trp, Anica. 2005. "An Experimental and Numerical Investigation of Heat Transfer during Technical Grade Paraffin Melting and Solidification in a Shell-and-Tube Latent Thermal Energy Storage Unit." In *Solar Energy*, 79:648–60. https://doi.org/10.1016/j.solener.2005.03.006.

Ukrainczyk, Neven, Juraj Sipusic, N Ukrainczyk, S Kurajica, and J Šipušiae. 2010. "Thermophysical Comparison of Five Commercial Paraffin Waxes as Latent Heat Storage Materials Multiscale Modeling of Advanced Nano-Reinforced Geopolymer/CNTs Materials View Project Advanced Short Course: 'COMPUTATIONAL METHODS FOR BUILDING PHYSICS AND CONSTRUCTION MATERIALS-LITE VERSION' View Project Thermophysical Comparison of Five Commercial Paraffin Waxes as Latent Heat Storage Materials." https://doi.org/10.15255/CABEQ.2014.240.